COVARIANT DENSITY FUNCTIONAL THEORY WITH SPECTROSCOPIC PROPERTIES IN NUCLEAR PHYSICS

P. Ring[1], G. A. Lalazissis[2], Z. P. Li[3], J. Meng[3], T. Niksic[4], L. Prochniak[5], D. Vretenar[4], J. M. Yao[6]

[1] *Physics Department Technical* University of Munich, *Garching, Germany*
[2] *Physics Department, Aristotle University of Thessaloniki, Greece*
[3] *School of Physics, Peking University, Beijing, China*
[4] *Physics Department, Faculty of Science, University of Zagreb, Croatia*
[5] *Physics Department, Maria Curie-Sklodowska University, Lublin, Poland*
[6] *School of Physical Science, Southwest University, Chongqing, China*

Covariant density functional theory (CDFT) is extremely useful for the investigation of ground state properties of nuclei all over the periodic table. For the calculations of nuclear spectra the generator coordinate method (GCM) is used to perform configuration mixing of angular-momentum projected wave functions generated by constrained self-consistent relativistic mean-field calculations. In this way correlations related to the restoration of broken symmetries and to fluctuations of collective variables are included. Because of the numerical complexity of such calculations, additional approximations are implemented to derive, in a fully microscopic way, the parameters of a five-dimensional collective Bohr Hamiltonian for vibrational and rotational degrees of freedom. This allows the calculations of nuclear spectra and it provides a microscopic theory of quantum phase transitions in finite nuclei.

1. Introduction

Nuclear density functional theories provide at present the only microscopic approaches to the nuclear many-body problem, that can be used over the whole nuclear chart, from relatively light systems to super-heavy nuclei, and from the valley of β-stability to the particle drip-line [1, 2]. The simplest implementation of this framework is based on the self-consistent mean-field approach. Here the density functional depends on the one-body density matrix that corresponds to a single product state. In this approach the many-body problem is effectively mapped onto a one-body problem, and the exact density functional is approximated by a functional of powers and gradients of ground-state nucleon densities and currents, representing distributions of matter, spins, momentum and kinetic energy. In principle this version can incorporate short-range correlations related to the repulsive core of the inter-nucleon interaction, and long-range correlations mediated by nuclear resonance modes.

The static density functional theory on the mean field level is characterized by symmetry breaking and can only provide an approximate description of bulk ground-state properties. To calculate excitation spectra and electromagnetic transition rates in individual nuclei, it is necessary to extend this framework to include collective correlations related to the restoration of broken symmetries and to fluctuations of collective coordinates.

In recent years several accurate and efficient models and algorithms have been developed that perform the restoration of symmetries broken by the static nuclear mean field, and take into account fluctuations around the mean-field minimum. The most effective approach to configuration mixing calculations is the generator coordinate method [3]. With the simplifying assumption of axial symmetry, GCM configuration mixing of angular-momentum, and even particle-number projected quadrupole-deformed mean-field states, has become a standard tool in nuclear structure studies with Skyrme energy density functionals [1], the density-dependent Gogny force [4], and relativistic density functionals [5, 6]. A variety of structure phenomena have been analyzed using this approach, for instance, the structure of low-spin deformed and superdeformed collective states [7, 8], shape coexistence in Kr and Pb isotopes [9, 10], shell closures in the neutron-rich Ca, Ti and Cr isotopes [11] and shape transition in Nd isotopes [12, 13]. Much more involved and technically difficult is the description of intrinsic quadrupole modes including triaxial deformations.

Only very recently fully microscopic three-dimensional calculations have been presented for Skyrme [14] and Gogny [15] mean field models generated by triaxial quadrupole constraints that are projected and mixed by the generator coordinate method. This method is actually equivalent to a seven-dimensional GCM calculation, mixing all five degrees of freedom of the quadrupole operator and the gauge angles for protons and neutrons. Here we report on configuration mixing of angular-momentum projected triaxial relativistic mean-field wave functions based on covariant density functionals [16].

2. The relativistic generator coordinate method

The generator coordinate method is based on the assumption that, starting from a set of mean-field states $|\Phi(q)\rangle$ which depend on collective coordinates q, one can build approximate eigenstates of the nuclear Hamiltonian by linear combination of such states:

$$|\Psi_\alpha\rangle = \int dq f_\alpha(q)|\Phi(q)\rangle$$

Detailed discussions of the GCM method can be found in Ref. [3]. To be able to compare theoretical predictions

with data, it is necessary to construct states with good angular momentum

$$|\Psi_\alpha^{JM}\rangle = \int dq \sum_{K\geq 0} f_\alpha^{JK}(q) \frac{1}{(1+\delta_{K0})} |JMK+,q\rangle$$

α labels collective eigenstates for a give angular momentum J. The details of the 3D angular-momentum projection in the relativistic case are given in Ref. [17]. The basis states $|JMK+,q\rangle$ are projected from the intrinsic wave functions $|\Phi(q)\rangle$:

$$|JMK+,q\rangle = [\hat{P}_{MK}^J + (-1)^J \hat{P}_{M-K}^J]|\Phi(q)\rangle$$

$\hat{P}_{MK}^J$ is the angular-momentum projection operator:

$$\hat{P}_{MK}^J = \frac{2J+1}{8\pi^2} \int d\Omega D_{MK}^{J*}(\Omega)\hat{R}(\Omega).$$

Ω denotes the set of three Euler angles and $D_{MK}^J(\Omega)$ are the Wigner functions [18]. The set of intrinsic wave functions $|\Phi(q)\rangle$, with the generic notation for quadrupole deformation parameters $q = (\beta, \gamma)$, is generated by imposing constraints on the axial q_{20} and triaxial q_{22} mass quadrupole moments in self-consistent RMF + BCS calculations. The following calculations are based on the relativistic point coupling model PC-F1 [19]:

$$E_{RMF} = \int dr \mathcal{E}_{RMF}(r) = \sum_k \int dr v_k^2 \bar{\psi}_k(r)(-i\gamma\nabla + m)\psi_k(r) +$$

$$+ \int dr \left(\frac{\alpha_S}{2}\rho_S^2 + \frac{\beta_S}{3}\rho_S^3 + \frac{\gamma_S}{4}\rho_S^4 + \frac{\delta_S}{2}\rho_S\Delta\rho_S + \frac{\alpha_V}{2}j_\mu j^\mu + \frac{\gamma_V}{4}(j_\mu j^\mu)^2 + \frac{\delta_V}{2}j_\mu\Delta j^\mu +\right.$$

$$\left. + \frac{\alpha_{TV}}{2}j_{TV}^\mu (j_{TV})_\mu + \frac{\delta_{TV}}{2}j_{TV}^\mu \Delta(j_{TV})_\mu + \frac{\alpha_{TS}}{2}\rho_{TS}^2 + \frac{\delta_{TS}}{2}\rho_{TS}\Delta\rho_{TS} + e\frac{1-\tau_3}{2}\rho_V A^0\right),$$

where $\psi(r)$ denotes a Dirac spinor. The local isoscalar and isovector densities and currents

$$\rho_S(r) = \sum_{k>0} v_k^2 \bar{\psi}_k(r)\psi_k(r),$$

$$\rho_{TS}(r) = \sum_{k>0} v_k^2 \bar{\psi}_k(r)\tau_3\psi_k(r),$$

$$j^\mu(r) = \sum_{k>0} v_k^2 \bar{\psi}_k(r)\gamma^\mu\psi_k(r),$$

$$j_{TV}^\mu(r) = \sum_{k>0} v_k^2 \bar{\psi}_k(r)\gamma^\mu\tau_3\psi_k(r)$$

are calculated in the *no-sea* approximation, i.e., the summation runs over all occupied states in the Fermi sea. The occupation factors v_k^2 of each orbit are determined in the simple BCS approximation, using a δ-pairing force. The pairing contribution to the total energy is given in the this case by

$$E_{\text{pair}}[\kappa,\kappa^*] = -\sum_{\tau=n,p} \frac{V_\tau}{4} \int d^3r \kappa_\tau^*(r)\kappa_\tau(r),$$

where V_τ is a constant pairing strength, and $\kappa(r)$ is the pairing tensor.

The weight functions $f_\alpha^{JK}(q)$ in the collective GCM wave function are determined from the variation:

$$\delta E^J = \delta \frac{\langle\Psi_\alpha^{JM}|\hat{H}|\Psi_\alpha^{JM}\rangle}{\langle\Psi_\alpha^{JM}|\Psi_\alpha^{JM}\rangle} = 0,$$

i.e., by requiring that the expectation value of the energy is stationary with respect to an arbitrary variation δf_α^{JK}. This leads to the Hill-Wheeler-Griffin (HWG) integral equation [20]:

$$\int dq' \sum_{K'\geq 0} [\mathcal{H}_{KK'}^J(q,q') - E_\alpha^J \mathcal{N}_{KK'}^J(q,q')] f_\alpha^{JK'}(q') = 0,$$

With the angular-momentum projected GCM kernel matrices of the Hamiltonian and the norm, respectively. The

Hamiltonian overlap can be evaluated in coordinate space,

$$H^J_{KK'}(q,q') = \int dr H^J_{KK'}(\boldsymbol{r};q,q'),$$

where

$$H^J_{KK'}(\boldsymbol{r};q,q') = \frac{2J+1}{8\pi^2}\int d\Omega D^{J*}_{KK'}\,\mathcal{H}(\boldsymbol{r};q,q';\Omega)n(q,q';\Omega)$$

and the norm overlap is defined by:

$$n(q,q';\Omega) \equiv \langle\Phi(q)|\hat{R}(\Omega)|\Phi(q')\rangle.$$

The calculation of the overlap matrix elements for the Hamiltonian is simplified by the generalized Wick theorem [21] that states that the Hamilton overlap matrix elements have the same form as the mean field functional, with the intrinsic single particle density matrix elements replaced by the corresponding transition density matrix elements [22].

The first step in the solution of the HWG matrix eigenvalue equation is the diagonalization of the norm overlap kernel

$$\sum_j \mathcal{N}^J(i,j)u^J_k(j) = n^J_k u^J_k(i).$$

From the eigenfunctions $u^J_k(i)$, also called "*natural states*", one builds the collective Hamiltonian

$$\mathcal{H}^J_{k\ell} = \frac{1}{\sqrt{n^J_k}}\frac{1}{\sqrt{n^J_\ell}}\sum_{i,j} u^J_k(i)\,\mathcal{H}^J(i,j)u^J_\ell(j),$$

which is subsequently diagonalized

$$\Sigma_\ell \mathcal{H}^J_{k\ell} g^{J\alpha}_\ell = E^J_\alpha g^{J\alpha}_k.$$

The solution of this eigenvalue equation determines both the energies E^J_α and the amplitudes $f^{JK}_\alpha(q)$ of collective states with good angular momentum Ψ^{JM}_α

$$f^{JK}_\alpha(q) = \sum_k \frac{g^{J\alpha}_k}{\sqrt{n^J_k}} u^J_k(i).$$

The weight functions $f^{JK}_\alpha(q)$ are not orthogonal and therefore cannot be interpreted as collective wave functions for the deformation variables. The collective wave functions $g^J_\alpha(i)$ are calculated from the norm overlap eigenstates:

$$g^J_\alpha(i) = \sum_k g^{J\alpha}_k\, u^J_k(i)$$

$g^J_\alpha(i)$ are orthonormal and, therefore, $|g^J_\alpha(i)|^2$ can be interpreted as a probability amplitude.

3. The low spin spectrum of ^{24}Mg

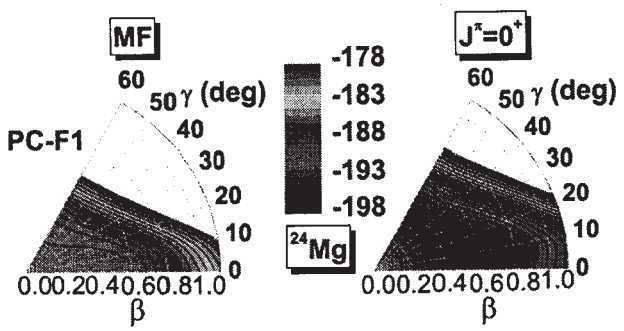

Fig. 1. Self-consistent RMF + BCS energy surface (*left* panel) of ^{24}Mg in the β-γ plane and angular momentum projected energy surface with $J = 0$ (*right* panel). The contours join points on the surface with the same energy. The difference between neighboring contours is 1.0 MeV.

Now we show several illustrative configuration mixing calculations in the nucleus ^{24}Mg. The intrinsic wave functions have been obtained as solutions of the self-consistent relativistic mean-field equations, subject to constraint on the triaxial mass quadrupole moments.

Fig. 1 shows the self-consistent RMF + BCS triaxial energy surface in the β-γ plane, The panel on the right displays the projected energy surface with $J = 0$. The energy surfaces nicely illustrate the effects of including triaxial shapes and of the restoration of rotational symmetry. The mean-field energy surfaces are found to be quite soft with a minimum at an axial prolate deformation $\beta = 0.5$. Projection shifts the minimum to a triaxial shape with $\beta = 0.5$ and $\gamma = 20°$. The gain in energy from the restoration of rotational

symmetry is 4.266 MeV. The fact that angular momentum projection leads to triaxial minima in the PES was already been noted in 3DAMP calculations in the eighties [24] and very similar results have been obtained recently using the Skyrme functional SLy4 [10].

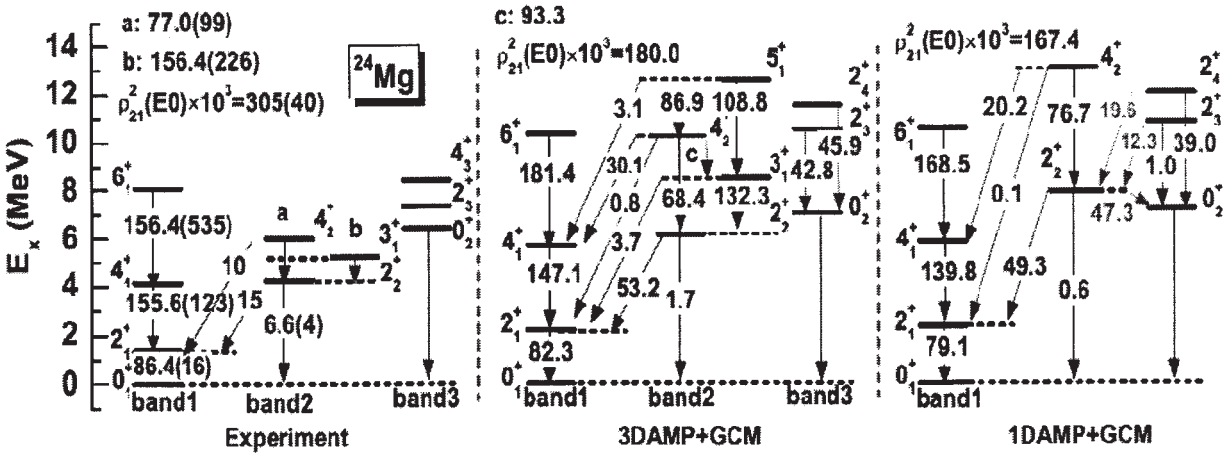

Fig. 2. The low-spin level scheme of ^{24}Mg calculated using the 3DAMP + GCM model and 1DAMP + GCM in comparison with data [28 - 30] The B(E2) values are given in units of e^{2}fm^4.

Fig. 2 displays the spectrum of the nucleus ^{24}Mg, calculated with the 3DAMP + GCM and 1DAMP + GCM codes. The 3DAMP + GCM and 1DAMP + GCM calculations produce virtually identical results. The level scheme is in rather good agreement with data, but in both cases the calculated spectra are systematically stretched as compared to experimental bands. This is because angular-momentum projection is performed only after variation and, therefore, time-odd components and alignment effects are neglected. Cranking calculations, for instance, correspond to an approximate angular-momentum projection before variation [25], and lead to an enhancement of the moments of inertia in better agreement with data [26, 27]. The agreement of the calculated quadrupole transition probabilities with data in is remarkable, especially considering that the calculation of B(E2) values is parameter-free, i.e. the transitions are calculated employing bare proton charges.

The nucleus ^{24}Mg presents an illustrative test case for the 3DAMP + GCM approach to low-energy nuclear structure. However, collective phenomena are, of course, much more pronounced in heavy nuclei and, therefore, the goal is to eventually apply the present approach to rare earth nuclei and the actinide region.

Axially symmetric AMP+GCM calculations are at present routinely performed for heavy nuclei [5], and from such studies one can estimate that N_{sh} = 16 shells have to be included in the oscillator basis for the systems in the mass region around Pb. Note that the computing time necessary for the evaluation of one overlap matrix element scales approximately with N_{sh}^6. These considerations show that a straightforward application of the existing 3DAMP + GCM codes to heavy nuclei is at the moment not possible. On the other hand, the introduction of additional approximations can considerably reduce the computing requirements. For instance, the overlap functions are strongly peaked at $q = q'$, and the use of Gaussian overlap approximations has produced excellent results in many cases. These approximations form the basis for the derivation of a collective Bohr Hamiltonian for quadrupole degrees of freedom [31, 32] discussed in the next section.

4. Derivation of a collective Bohr Hamiltonian in 5 dimensions

In an alternative approach to five-dimensional quadrupole dynamics that includes rotational symmetry restoration and takes into account triaxial quadrupole fluctuations, a collective Bohr Hamiltonian is constructed, with deformation-dependent parameters determined from microscopic self-consistent mean-field calculations. The collective Hamiltonian can be derived in the Gaussian overlap approximation (GOA) [3] to the full five-dimensional GCM. With the assumption that the GCM overlap kernels can be approximated by Gaussian functions, the local expansion of the kernels up to second order in the non-locality transforms the GCM Hill-Wheeler equation into a second-order differential equation - the Schrödinger equation for the collective Hamiltonian. The kinetic part of this Hamiltonian contains an inertia tensor and the potential energy is determined by the diagonal elements of the Hamiltonian kernel, and also includes zero-point energy (ZPE) corrections. The adiabatic time-dependent Hartree-Fock (ATDHF) theory [33] provides an alternative way to derive a classical collective Hamiltonian and, after re-quantization, a Bohr Hamiltonian of the same structure is obtained, but with different microscopic expressions for the inertia parameters.

Here we discuss a new implementation for the solution of a five-dimensional collective Hamiltonian that describes quadrupole vibrational and rotational degrees of freedom, with parameters determined in the framework of covariant density functional theory. An initial study along this line was reported in Ref. [41].

The three terms of the classical collective Hamiltonian, expressed in terms of the intrinsic variables β, γ and Euler angles

$$H_{\rm coll} = \mathcal{T}_{vib}(\beta,\gamma) + \mathcal{T}_{rot}(\beta,\gamma,\Omega) + \mathcal{V}_{coll}(\beta,\gamma)$$

denote the contributions from the vibrational kinetic energy:

$$\mathcal{T}_{vib} = \frac{1}{2}\boldsymbol{B}_{\beta\beta}\dot{\beta}^2 + \beta\boldsymbol{B}_{\beta\gamma}\dot{\beta}\dot{\gamma} + \frac{1}{2}\beta^2\boldsymbol{B}_{\gamma\gamma}\dot{\gamma}^2$$

the rotational kinetic energy:

$$\mathcal{T}_{rot} = \frac{1}{2}\sum_{k=1}^{3}\mathcal{I}_k\,\omega_k^2,$$

and the collective potential energy $\mathcal{V}_{coll}(\beta,\gamma)$. The mass parameters $\boldsymbol{B}_{\beta\beta}$, $\boldsymbol{B}_{\beta\gamma}$, and $\boldsymbol{B}_{\gamma\gamma}$ and the moments of inertia $\mathcal{I}_k$ depend on the quadrupole deformation variables β and γ.

This Hamiltonian is quantized according to the general Pauli prescription:

$$\hat{H}_{kin} = -\frac{\hbar^2}{2}\frac{1}{\sqrt{\det B}}\sum_{ij}\frac{\partial}{\partial q_i}\sqrt{\det B}\,(B^{-1})_{ij}\frac{\partial}{\partial q_j}.$$

The potential energy contains in addition to the mean field potential $V(q)$ correction terms for the zero point energies of vibrations and rotations.

The single-nucleon wave functions, energies and occupation factors, generated from constrained self-consistent solutions of the RMF+BCS equations, provide the microscopic input for the parameters of the collective Hamiltonian. We use for the rotational moments of inertia the Inglis - Belyaev formula

$$\mathcal{I}_k = \sum_{i,j}\frac{(u_i v_j - v_i u_j)^2}{E_i + E_j}\left|\langle \mathrm{i}|\hat{J}_k|\mathrm{j}\rangle\right|^2 \qquad k = 1,2,3,$$

and for mass parameters of the vibrational degrees of freedom the Cranking approximation

$$B_{\mu\nu}(q_0,q_2) = \frac{\hbar^2}{2}\left[\mathcal{M}_{(1)}^{-1}\mathcal{M}_{(3)}\mathcal{M}_{(1)}^{-1}\right]_{\mu\nu},$$

where

$$\mathcal{M}_{(n),\mu\nu}(q_0,q_2) = \sum_{i,j}\frac{\langle \mathrm{i}|\hat{Q}_{2\mu}|\mathrm{j}\rangle\langle \mathrm{j}|\hat{Q}_{2\nu}|\mathrm{i}\rangle}{(E_i + E_j)^n}(u_i v_j - v_i u_j)^2.$$

Further details are given in Ref. [31].

5. A microscopic theory of quantum phase transitions in finite nuclei

The evolution of shell structures governs the variation of ground-state nuclear shapes along isotopic and isotonic chains. Nuclear structure explores a variety of phenomena related to structural evolution including, for instance, the reduction of spherical shell gaps and modifications of magic numbers in nuclei far from stability, occurrence of islands of inversion and coexistence of shapes with different deformations. As the number of nucleons changes from nucleus to nucleus, in general one observes a gradual evolution of different shapes - spherical, axially deformed, shapes that are soft with respect to triaxial deformations. These shape transitions reflect the underlying modifications of single-nucleon shell structure and interactions between valence nucleons. An especially interesting feature is the possible occurrence of shape phase transitions and critical-point phenomena for particular values of the number of protons and neutrons. Phase transitions in the equilibrium shapes of nuclei correspond to first- and second order quantum phase transitions (QPT) between competing ground-state phases induced by variation of a non thermal control parameter (number of nucleons) at zero temperature. Nuclear quantum phase transitions have been the subject of extensive experimental and theoretical studies during the past decade. Recent reviews and an exhaustive bibliography can be found in Refs. [34, 35]. Even though phase transitions in finite systems can be defined only in the classical limit in which the number of constituents tends to infinity, i.e., the transition is actually smoothed out in finite systems, there are nevertheless clear experimental signatures of abrupt changes in structure properties of finite nuclei with the addition or subtraction of only few nucleons. This is another distinct feature of QPT in atomic nuclei, i.e., the physical control parameter, number of nucleons, can take only discrete integer values. Expectation values of suitably chosen operators, that as observables characterize the state of a nuclear system, can be used as order parameters [9]. Theoretical studies of nuclear QPT are typically based on macroscopic geometric models of nuclear shapes and potentials [36] and/or semi-microscopic algebraic models [35]. In the geometric framework QPT's are analyzed in terms of a Bohr collective Hamiltonian for shape variables and can be related to the concept of critical-point symmetries that provide parameter-independent predictions for excitation spectra and

electromagnetic transition rates for nuclei at the phase transition point. Alternatively, in the algebraic approach [e.g., the interacting boson model (IBM)] different shapes coincide with particular dynamical symmetries of some algebraic structure, and the phase transition occurs when these symmetries are broken in a specific way. The two frameworks can be related, for instance, by using the coherent state formalism that allows us to establish a correspondence between the symmetry limits of the algebraic Hamiltonian and energy functionals expressed in terms of collective shape variables. In both approaches, geometric and algebraic, the description of QPT is based on model-specific Hamiltonians that by construction describe shape changes. A shape phase transition is then accessed by variation of a control parameter. The two best-studied classes of nuclear shape phase transitions, both theoretically and experimentally, correspond to a second-order QPT between spherical and γ-soft shapes and a first-order QPT between spherical and axially deformed shapes [37 - 38]. The former is a phase transition in one degree of freedom (the axial deformation β) and, in the IBM language, represents a transition between the U(5) and SU(3) dynamical symmetries in the limit of large boson number. The critical point of this phase transition, denoted X(5), does not correspond to a dynamical symmetry in the usual sense. Nevertheless, for the particular case in which the β and γ degrees of freedom are decoupled, an approximate analytic solution at the critical point of phase transition can be expressed in terms of zeros of Bessel functions of irrational order [37]. Evidence for the empirical realization of X(5) phase transition was first reported for ^{152}Sm and other N = 90 isotones in Ref. [38]. Even though phenomenological approaches to nuclear QPT have been very successful, and the predicted isotopic trends for various observables are in very good agreement with data, it would clearly be desirable to have a fully microscopic description of shape phase transitions, starting from nucleonic degrees of freedom. This is especially important in view of the fact that the physical control parameter in nuclear QPT is the actual number of nucleons in a nucleus, rather than a strength parameter of a model-specific, Ising-type Hamiltonian. Several recent studies have reported microscopic calculations of potential energy surfaces as functions of quadrupole deformation, for a number of isotopic chains in which the occurrence of shape phase transitions had been predicted. Potentials calculated with a constraint on the mass quadrupole moment display shape transitions from spherical to deformed configurations.

In Ref. [12] have we analyzed shape transitions in Nd isotopes, using the microscopic model based on relativistic density functional PC-F1. Starting from constrained self-consistent mean-field calculations of potential energy curves, the one-dimensional generator coordinate method (GCM) was used to perform configuration mixing of angular-momentum and particle-number projected relativistic wave functions. It was shown that the microscopic framework based on universal density functionals, adjusted to nuclear ground-state properties and extended to take into account correlations related to symmetry restoration and fluctuations of collective variables, describes not only general features of shape transitions but also the unique behavior of excitation spectra and transition rates at the critical point of quantum shape phase transition. In particular, the particle-number projected GCM spectra, intra-band and inter-band B(E2) values for ^{148,150,152}Nd were found in excellent agreement with data and close to the X(5)-model predictions for ^{150}Nd. The self-consistent GCM calculation based on the relativistic density functional PC-F1 predicted the shape phase transition precisely at the isotope ^{150}Nd, in agreement with empirical evidence for the realization of X(5) in the N = 90 rare-earth isotones. X(5) denotes a particular model for a first-order QPT between spherical and axially deformed shapes, based on the assumption of a separable potential $V_{\beta\gamma}(\beta\gamma) = V_\beta(\beta) + V_\gamma(\gamma)$.

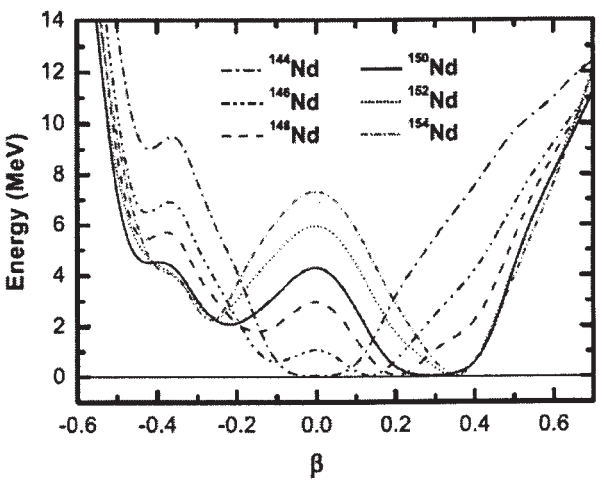

Fig. 3. Self-consistent RMF + BCS potential energy curves of the even-even Nd-isotopes as function of deformation parameter β. The energies are normalized with respect to the absolute minimum for a given isotope.

Here we discuss a treatment of this phase transitions in a 3D model allowing for triaxial shapes [32]. Collective excitation spectra and transition probabilities are calculated starting from a five-dimensional collective Hamiltonian for quadrupole vibrational and rotational degrees of freedom, with parameters determined by constrained self-consistent relativistic mean field calculations with the covariant density functional PC-F1 [19]. Fig. 3 shows the mean field potential energy curves for vanishing γ-deformation. Of course, these curves are more realistic than the infinite square well considered by Iachello in Ref. [37]. First, although it displays a wide flat minimum in β on the prolate side, the flat bottom of the potential does not start at $\beta = 0$, i.e., the coexisting shapes do not include the spherical configuration. In this respect the microscopic potential is closer to the generalization of the axially symmetric X(5) solution for the collective Bohr Hamiltonian to the transition path between X(5) and the rigid-rotor limit, represented by infinite square-well potentials over a confined range of β-values [39]. Second, the microscopic potential well has softer walls compared to the X(5) square well. For the rotational moments of inertia of the collective Hamiltonian we have multiplied the Inglis - Belyaev values with a common factor determined in such a way that the calculated energy of the 2^+_1 state coincides

with the experimental value. In deformed nuclei, to a good approximation, the enhancement of the effective moment of inertia scales with the relative excitation energies within each band by a common factor but otherwise leaves the band head of the β-band (0^+_2) unaltered. Of course, this simple relation between the scaling of effective moments of inertia and excitation energies within each band would be exact only if rotational and vibrational degrees of freedom were decoupled.

The inclusion of an additional scale parameter in the calculation was necessary because of the well-known fact that the Inglis - Belyaev (IB) formula predicts effective moments of inertia that are considerably smaller than empirical values. More realistic values are only obtained if one uses the Thouless - Valatin (TV) formula, but this procedure is computationally much more demanding, and it has not been implemented in the current version of the model.

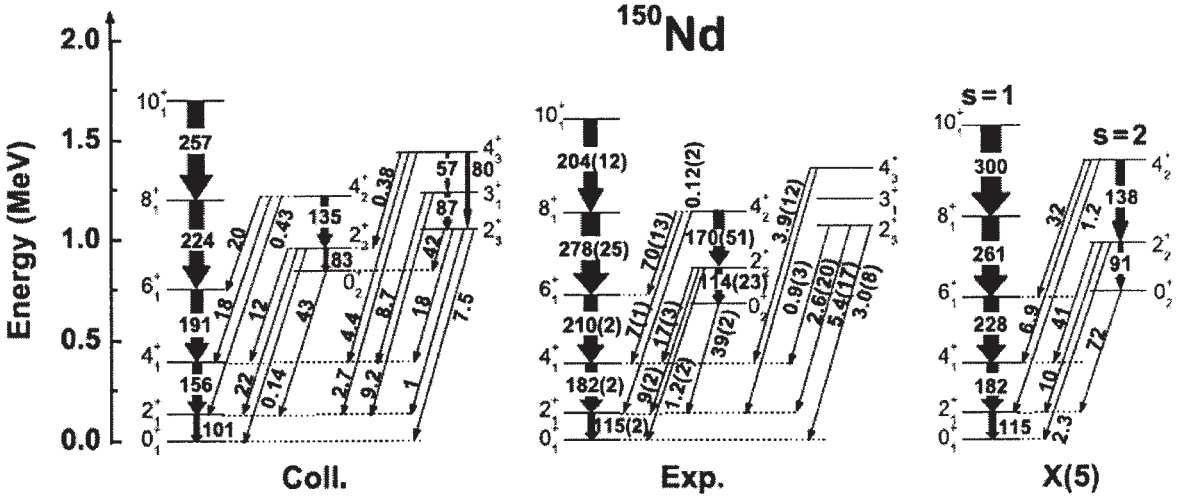

Fig. 4. The spectrum of ^{150}Nd derived from covariant density functional (*left*) and compared with data [40] (*middle*) and the X(5)-symmetry predictions (*right*). The intra-band and inter-band B(E2) values are given in W.u.). The theoretical spectra are normalized to the experimental energy of the state 2^+_1 and the X(5) transition strengths are normalized to the experimental B(E2; $2^+_1 \rightarrow 0^+_1$) value.

The resulting excitation spectrum of ^{150}Nd, calculated with the PC-F1 density functional, and the corresponding intra-band and inter-band B(E2) values, are in good agreement with available data for the ground-state band and the β- and γ-bands, see Fig. 4. The calculation reproduces the excitation energies of the band heads 0^+_2 and 2^+_3 of the β- and γ-bands, respectively, and, when the Inglis - Belyaev effective moments of inertia are renormalized to the empirical value, also the relative excitation energies in all three bands. The parameter-free predictions for the B(E2)'s reproduce the experimental values not only for intra-band transitions within the ground-state band and the β-band but also for transitions from the β- and γ-bands to the ground-state band, including the measured branching ratios.

5. Summary and outlook

Among the microscopic approaches to the nuclear many-body problem, the framework of nuclear density functional theory provides the most complete description of ground-state properties and collective excitations over the whole nuclide chart. The self-consistent mean-field models based on the density functional framework describe not only general features of shape transitions but also particular properties of spectra and transition rates at the critical point of the QPT. However, to calculate excitation spectra and transition probabilities, the self-consistent mean-field approach has to be extended to include correlations related to restoration of broken symmetries and fluctuations of collective variables. This can be done either by performing GCM configuration mixing calculations of projected wave functions or by constructing collective Bohr-type Hamiltonians with deformation-dependent parameters determined from self-consistent mean-field calculations. The possibility to perform self-consistent microscopic studies of shape transitions opens a new perspective on the origin of nuclear QPT in various mass regions. It is therefore important to systematically analyze, also employing different energy-density functionals, various types of shape phase transitions that have been predicted in several regions of medium-heavy and heavy nuclei.

Acknowledgements

This work was partly supported by the DFG cluster of excellence *Origin and Structure of the Universe* (www.universe-cluster.de).

REFERENCES

1. *Bender M., Heenen P.-H., Reinhard P.-G.* // Rev. Mod. Phys. - 2003. - Vol. 75. - P. 121.
2. *Vretenar D., Afanasjev A.V., Lalazissis G.A., Ring P.* // Phys. Rep. - 2005. - Vol. 409. - P. 101.
3. *Ring P., Schuck P.* The nuclear many-body problem. - New York: Springer Verlag, 1980.
4. *Rodriguez-Guzman R., Egido J. L., Robledo L. M.* // Nucl. Phys. - 2002. - Vol. A709. - P. 201.
5. *Niksic T., Vretenar D., Ring P.* // Phys. Rev. - 2006. - Vol. C73. - P. 034308.
6. *Niksic T., Vretenar D., Ring P.* // Phys. Rev. - 2006. - Vol. C74. - P. 064309.
7. *Rodriguez-Guzman R., Egido J.L., Robledo L.M.* // Phys. Rev. - 2000. - Vol. C62. - P. 054308.
8. *Bender M., Flocard H., Heenen P.-H.* // Phys. Rev. - 2003. - Vol. C68. - P. 044321.
9. *Rodriguez-Guzman R., Egido J.L., Robledo L.M.* // Phys. Rev. - 2004. - Vol. C69. - P. 054319.
10. *Bender M., Flocard H., Heenen P.-H.* // Phys. Rev. - 2006. - Vol. C74. - P. 024312.
11. *Rodriguez T.R., Egido J.L.* // Phys. Rev. Lett. - 2007. - Vol. 99. - P. 062501.
12. *Niksic T., Vretenar D., Lalazissis G.A., Ring P.* // Phys. Rev. Lett. - 2007. - Vol. 99. - P. 092502.
13. *Rodriguez T.R., Egido J.L.* // Phys. Lett. - 2008. - Vol. B663. - P. 49.
14. *Bender M., Heenen P.-H.* // Phys. Rev. - 2008. - Vol. C78. - P. 024309.
15. *Rodriguez T.R., Egido J.L.* // arXiv:1004.2877v1 [nucl-th]
16. *Yao J. M., Meng J., Ring P., Vretenar D.* // Phys. Rev. - 2010. - Vol. C81. - P. 044311.
17. *Yao J. M., Meng J., Ring P., Pena Arteaga D.* // Phys. Rev. - 2009. - Vol. C79. - P. 044312.
18. *Edmonds A.R.* Angular Momentum in Quantum Mechanics. - Princeton: University Press, 1957.
19. *Bürvenich T., Madland, D.G., Maruhn J.A,, Reinhard P.-G.* // Phys. Rev. - 2002. - Vol. C65. - P. 044308.
20. *Hill D.L., Wheeler J.A.* // Phys. Rev. - 1953. - Vol. 89. - P. 1102.
21. *Balian R., Brezin E.* // Nuovo Cim. - 1969. - Vol. 64B. - P. 37.
22. *Onischi N., Yoshida S.* // Nucl. Phys. - 1966. - Vol. 80. - P. 367.
23. *Koepf W., Ring P.* // Phys. Lett. - 1988. - Vol. B212. - P. 397.
24. *Hara, K., Hayashi A., Ring P.* // Nucl. Phys. - 1982 - Vol. A385. - P. 14.
25. *Beck, R., Mang H.-J., Ring P.* // Z. Phys. - 1970 - Vol. 231. - P. 26.
26. *Koepf W., Ring P.* // Nucl. Phys. - 1989. - Vol. A493. - P. 61.
27. *Afanasjev A. V. et al.* // Phys. Rev. - 2000. - Vol. C62. - P. 054306.
28. *Endt P. M.* // At. Data Nucl. Data Tables. - 1993. - Vol. 55. - P. 171.
29. *Branford D., McGough A.C., Wright I.F.* // Nucl. Phys. - 1975. - Vol. A241. - P. 349.
30. *Keinonen J. et al.* // Nucl. Phys. - 1989. - Vol. A493. - P. 124.
31. *Niksic T., Li Z.P., Vretenar D. et al.* // Phys. Rev. - 2009. - Vol. C79. - P. 034303.
32. *Li Z.P., Niksic T., Vretenar D. et al.* // Phys. Rev. - 2009. - Vol. C79. - P. 054301.
33. *Baranger M., Veneroni M.* // Ann. Phys. (N. Y.) - 1978 - Vol. 114. - P. 123.
34. *Casten R.F.* // Nature Physics. - 2006. - Vol. 2. - P. 811.
35. *Ceynar P., Jolie J.* // Prog. Part. Nucl. Phys. - 2009. - Vol. 62. - P. 210.
36. *Iachello F., Zamfir N.Y.* // Phys. Rev. Lett. - 2004. - Vol. 92. - P. 212501.
37. *Iachello F.* // Phys. Rev. Lett. - 2001. - Vol. 87. - P. 052502.
38. *Casten R.F., Zamfir N.V.* // Phys. Rev. Lett. - 2001. - Vol. 87. - P. 052503.
39. *Piatralla N., Gorbachenko O.M.* // Phys. Rev. - 2004. - Vol. C70. - P. 011304(R).
40. *Krücken R. et al.* // Phys. Rev. Lett. - 2002. - Vol. 88. - P. 232501.
41. *Prochniak L., Ring P.* // Int. J. Mod. Phys. - 2004. - Vol. E13. - P. 217.